

Influence of Nickel-Based Alloys' Mechanical Properties on Mechanochemical Effect at Crack Tip in High Temperature Water Environments

Yang Fuqiang, Xue He, Zhao Lingyan, Fang Xiurong

Xi'an University of Science and Technology, Xi'an 710054, China

Abstract: Mechanochemical effect which is the mechanical and chemical interaction can accelerate the stress corrosion cracking (SCC) in nickel-based alloys used in nuclear power plants. The mechanical property heterogeneity in weld joints will influence the mechanochemical effect indirectly. The influences of yield strength and hardening exponent of nickel-based alloy 600 on the mechanochemical effect of crack tip surface in high temperature water environment were studied by adopting one inch compact tension specimen and finite element method. The influence of elastic and plastic deformation on the mechanochemical effect at crack tip was discussed. The results indicate that the mechanochemical effect is affected by the yield strength. In contrary, the hardening exponent change of alloy 600 has an insignificant influence on mechanochemical effect.

Key words: mechanochemical effect; yield strength; hardening exponent; crack tip; finite element

Although important equipments in nuclear power plants, such as reactor pressure vessel, steam generators, and pressurizers, are welded by nickel-based alloys which are heat-resistant and anti-corrosive, the safety of nuclear power is still threatened by stress corrosion cracking (SCC)^[1,2]. The quantitative prediction of SCC rate of nickel-based alloys in high temperature water considering the factors affecting SCC has been an important field of safety assessment of nuclear materials. During past 50 years, many SCC mechanisms and prediction models of nickel-based alloys and austenitic stainless steels in high temperature water had been summarized based on a large number of experimental studies^[3,4] which provided the guidance for the safety design and operation of nuclear power plants. Although many factors affecting SCC rates have been studied^[5,6], it is essential to comprehend the interactions among SCC factors in order to improve the accuracy of SCC model.

As one of the important interactions among SCC factors, the mechanochemical effect which explains the relationship

between stress and the electrochemical corrosion environment of SCC, shows that the electrochemical corrosion potential (ECP) of metals will migrate if elastic or plastic deformation occurs^[7-9]. It is proved that SCC occurs only in a critical potential range, a tiny disturbance of the potential may change the metal surface status and leads to the variation of corrosion current density and corrosion rates, so the change of stress will accelerate corrosion rates in mechanical and electrochemical aspects simultaneously. The influences of material property differences of nickel-based alloys in heat-affected zone on crack tip stress and strain fields had been studied^[10-12], but the indirect influences of material property differences on the mechanochemical effect in SCC process are still unclear. In the present study, the influences of material property differences of nickel based alloy 600 on mechanochemical effect in SCC were discussed by a finite element method (FEM) and sub-model technology.

1 Theory Model

Received date: July 25, 2015

Foundation item: National Natural Science Foundation of China (51475362); Scientific Research Program Funded by Shaanxi Provincial Education Department (12JK0657); Research Fund for the Doctoral Program of Higher Education of China (20136121110001)

Corresponding author: Xue He, Ph. D., Professor, School of Mechanical Engineering, Xi'an University of Science and Technology, Xi'an 710054, P. R. China, Tel: 0086-29-83856250, E-mail: xue_he@hotmail.com

Copyright © 2016, Northwest Institute for Nonferrous Metal Research. Published by Elsevier BV. All rights reserved.

In the system with positive ions and influenced by mechanical and electrical factors simultaneously, the ECP change of metals is different under elastic or plastic deformation. The ECP change of elastic metals is related to the external pressure, and equals to the change of standard electrical potential^[7], as shown in the following equation:

$$\Delta\varphi_E = -\frac{\Delta PV_m}{zF} \quad (1)$$

where $\Delta\varphi_E$ is the change of equilibrium electrical potential caused by elastic deformation; ΔP is external excess pressure experienced by the metal, and it will be denoted by the absolute value of the hydrostatic part of stress tensor, and equals to hydrostatic pressure in Abaqus calculations; V_m is the mole volume of metal; Z is ion valence and F is Faraday's number.

The ECP change in plastic metals is the additional chemical potential of atoms caused by dislocation besides external pressure, and the ECP change caused by dislocation can be calculated by the following equation^[7]:

$$\Delta\varphi_p = -\frac{RT}{zF} \ln \frac{\varepsilon}{\varepsilon_0} \quad (2)$$

where $\Delta\varphi_p$ is the change of equilibrium electrical potential caused by plastic deformation; R is gas constant; T is absolute temperature; ε is the strain of material, and will be instead by equivalent plastic strain in Abaqus calculations; ε_0 corresponds to the onset of strain hardening.

The overall value of mechanochemical effect $\Delta\varphi$ is defined by the standard potential shift which represents a sum of Eq.(1) and Eq.(2):

$$\Delta\varphi = -\frac{1}{zF} \left[RT \ln \frac{\varepsilon}{\varepsilon_0} + \Delta PV_m \right] \quad (3)$$

The Eq.(3) will be used in plastic zone, and in contrary, the Eq.(1) will be used to calculate the ECP change in elastic zone.

2 FEM Simulations

2.1 Material and specimen model

One inch compact tension specimen (1T-CT) was used in this numerical calculation with the virtual experiment process according to the American Society for Testing and Materials Standard^[13]. The geometric shape and the size of 1T-CT specimen are shown in Fig.1. The non linear relationship between stress and strain beyond yield at crack tip of nickel-based alloys is described by Ramberg-Osgood equation in this numerical simulation^[14]:

$$\varepsilon = \frac{\sigma}{E} + \alpha \frac{\sigma_0}{E} \left[\frac{\sigma}{\sigma_0} \right]^m \quad (4)$$

where ε is strain; σ is stress; E is Young's modulus of the material; σ_0 is the yield strength of the material; α is the yield offset and m is the hardening exponent for the plastic deformation.

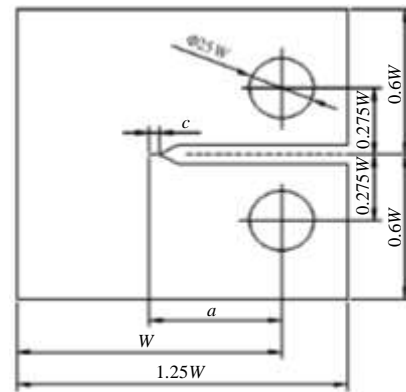


Fig.1 Geometric size of 1T-CT specimen ($W=50$ mm, $a=0.5W$, $c=1.5$ mm)

The study was divided into three stages with crack tip stress intensity factor being equal to $7 \text{ MPa m}^{1/2}$ constantly^[15]. Firstly, the alloy 600 at $288 \text{ }^\circ\text{C}$ was used as base metal, the mechanical properties of alloy 600 are given in Table 1^[15]. The yield strength and hardening exponent in Table 1 were regarded as reference value σ_0 and initial hardening exponent m_0 , respectively. Secondly, the yield strength of alloy 600 was arbitrarily set to $0.8\sigma_0$, $0.9\sigma_0$, $1.1\sigma_0$, and $1.2\sigma_0$ with other properties as constant to study the influences of yield strength change on mechanochemical effect. Thirdly, the hardening exponent of alloy 600 was arbitrarily changed to 4.495, 5.495, 7.495 and 8.495 with other properties unchanged to investigate its influence on mechanochemical effect.

The film, which was simplified as Cr_2O_3 at alloy 600 surface in PWR (pressurized-water reactor) primary water^[16], was assumed dissolving in front of crack and only left on sides of crack. This study focuses on the crack tip without film and the mechanochemical effect only affect the anodic dissolution current^[17]. The simulation parameters used in this study are listed in Table 2^[15].

Table 1 Mechanical properties of alloy 600 and passive film in PWR primary water at $288 \text{ }^\circ\text{C}$ ^[15]

Property	Alloy 600	Passive film
Yield strength, σ_0/MPa	436	810
Young's modulus, E/GPa	189.5	140
Yield offset, α	3.075	3.075
Hardening exponent, m	6.495	6.495
Poisson's ratio, ν	0.286	0.31

Table 2 Parameters used in simulation^[15]

Parameter	Value
Ion valence, Z	2
Faraday's number, $F/\text{C mol}^{-1}$	96 485.338 3
Mole volume of alloy 600, $V_m/\text{cm}^3 \text{ mol}^{-1}$	6.749 8
Gas constant, $R/\text{J K}^{-1} \text{ mol}^{-1}$	8.314 472
Absolute temperature, T/K	613.15

2.2 FE model

The loading process and the ECP changes were simulated by FE code ABAQUS adopting a 1T-CT specimen. A small size blunt notch with a radius of 0.5 μm was designed at the crack tip to obtain the stress and strain distribution in the vicinity of crack tip. A sub-model with 0.1 mm side length was created near the crack tip to improve the calculation accuracy. The passive film was only introduced in sub-model with the thickness of 2 μm to simplify the calculating process. The specimen was simplified as a plane strain model since the crack front along thickness of specimen is mainly dominated by the plane strain condition. The mesh of the specimen is shown in Fig.2, where the whole model and sub-model were meshed to 20 880 and 29 943 8-node biquadratic plane strain quadrilateral (CPE8) elements, respectively.

3 Results and Discussion

3.1 Stress and strain distribution on crack tip surface

The distributions of Von Mises stress σ_v on crack tip surface with different material properties are shown in Fig.3. It can be seen that the distribution trends of σ_v around crack tip are the same in spite of material properties change. The maximum σ_v appears at $\theta=0^\circ$ and decreases gradually with increasing of θ , while, the minimum σ_v appears at $\theta=90^\circ$. The σ_v around crack tip will increase with increasing of yield strength and decrease with increasing of hardening exponent.

Fig.4 indicates that the equivalent plastic strain ε_E of crack tip surface decreases from the front to the sides of crack gradually, but ε_E decreases with increasing of yield strength and increases with increasing of hardening exponent.

3.2 Hydrostatic pressure on crack tip surface

The influences of material property on the hydrostatic pressure around crack tip are shown in Fig.5. The hydrostatic pressures also have the maximum values at $\theta=0^\circ$ and decrease gradually as θ increases, but the hydrostatic pressures decrease sharply when $\theta>80^\circ$, and the smallest value appears at $\theta=90^\circ$. The hydrostatic pressure around crack tip are also affected by the mechanical properties of alloy 600. The hydrostatic pressure will increase with increasing of yield strength and decrease with the increasing of hardening exponent.

3.3 Influences of material properties on crack tip surface mechanochemical effect

The influences of material property changes on the distribution of crack tip surface ECP changes $\Delta\phi$ were calculated according to Eq.(1) and Eq.(3), and the results are shown in Fig.6. The ECP changes $\Delta\phi$ have maximum values at $\theta=0^\circ$, and decrease gradually upon θ increasing, while the minimum values appear at $\theta=90^\circ$. The values of $\Delta\phi$ decrease with increasing of yield strength, while the change of hardening exponent of alloy 600 has no significant influences on the value of $\Delta\phi$.

The sensitivities of ECP change with yield strength as shown in Fig.7. It can be seen that ECP change has the strongest sensitivity with yield strength, $\theta=90^\circ$, and decreases gradually as θ tends to 0° . In addition, it is found that the sensitivity curves almost coincide together from 0° to 90° with yield strength increasing of 10% and 20%, or with yield strength decreasing of 10% and 20%. This indicates that the distribution of ECP change has low sensitivity with the change amplitude of yield strength, but the decreasing of yield strength will affect the ECP value more evidently than its increasing.

Since the stresses around crack tip are larger than the yield strength of alloy 600, the crack tip is regarded as yield zone. Thus the ECP change $\Delta\phi$ is composed of elastic part $\Delta\phi_E$ and plastic part $\Delta\phi_P$. The changes of $\Delta\phi_E$ and $\Delta\phi_P$ with different yield strength of alloy 600 are shown in Fig.8. The value of $\Delta\phi_E$ is from 5 mV to 20 mV, while $\Delta\phi_P$ changes from 40 mV to 110 mV. The $\Delta\phi_E$ and $\Delta\phi_P$ have converse change trends when the yield strength changes. The value of $\Delta\phi_E$, which is affected only by hydrostatic pressure according to Eq.(1), has the same change trends with hydrostatic pressure, and increases with increasing of yield strength. The value of $\Delta\phi_P$ decreases with increasing of yield strength, which can be explained by Eq.(2) and Eq.(4). According to Eq.(4), the increase of yield strength will improve the yield strain ε_0 , simultaneously, the strain ε decreases when the yield strength of alloy 600 increases under the same load. This leads to the opposite variation of yield strength and $\Delta\phi_P$. As $\Delta\phi_P$ is much bigger than $\Delta\phi_E$, the total change of $\Delta\phi$ is dominated by $\Delta\phi_P$.

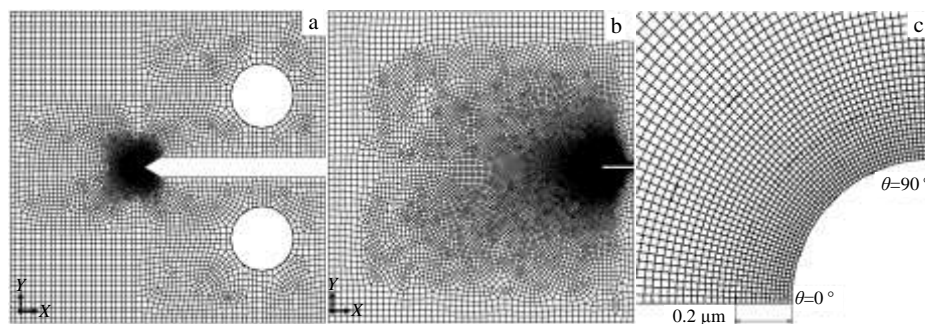


Fig.2 Mesh of the 1T-CT specimen (a), sub-model (b), and the detail around crack tip of sub-model (half) (c)

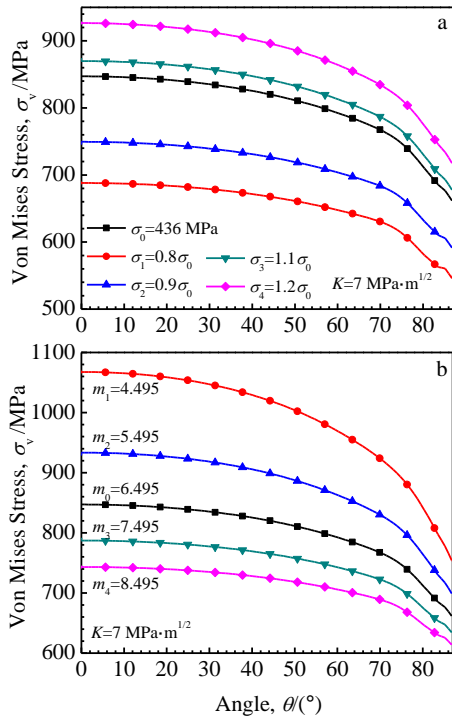


Fig.3 Von Mises stress distribution on crack tip surface of alloy 600 with different yield stresses (a) and hardening exponents (b)

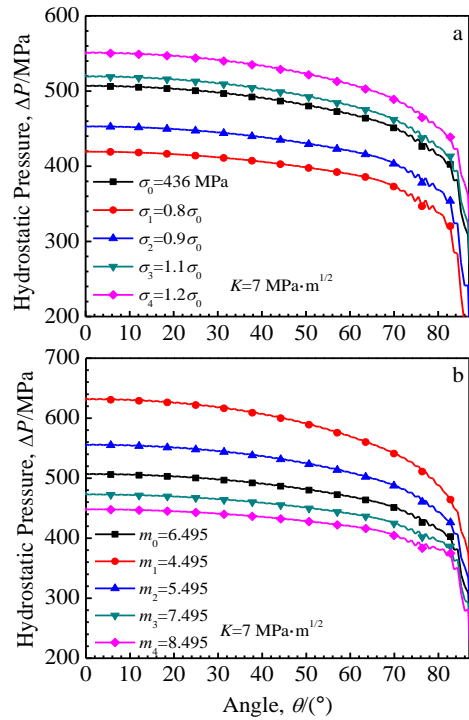


Fig.5 Hydrostatic pressure distribution on crack tip surface of alloy 600 with different yield stresses (a) and hardening exponents (b)

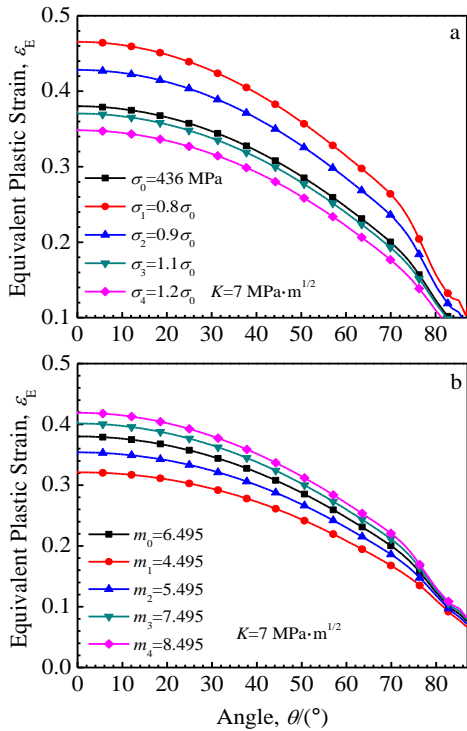


Fig.4 Equivalent plastic strain distribution on crack tip surface of alloy 600 with different yield stresses (a) and hardening exponents (b)

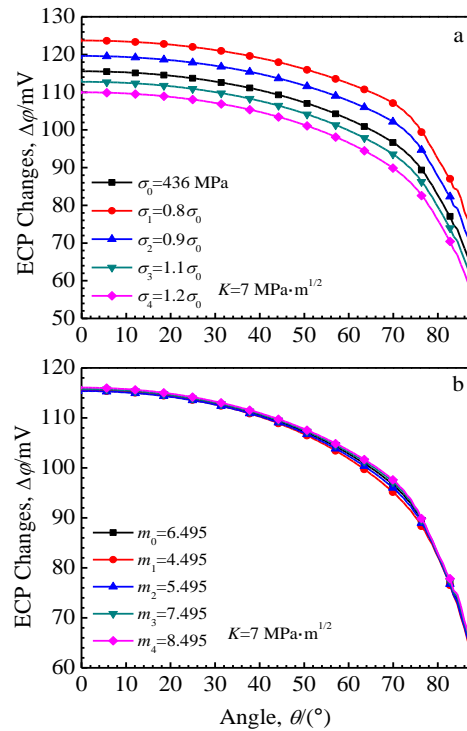


Fig.6 ECP distribution on crack tip surface of alloy 600 with different yield stresses (a) and hardening exponents (b)

The comparisons of $\Delta\phi_p$ and $\Delta\phi_E$ in Fig.9 show that $\Delta\phi_p/\Delta\phi_E$ has the maximum value at $\theta = 0^\circ$ and decreases

gradually with increasing of θ . This indicates that the closer the crack tip, the greater the proportion of $\Delta\phi_p$ in $\Delta\phi$. After a slightly apparent reduction at $\theta > 70^\circ$, $\Delta\phi_p/\Delta\phi_E$ increases

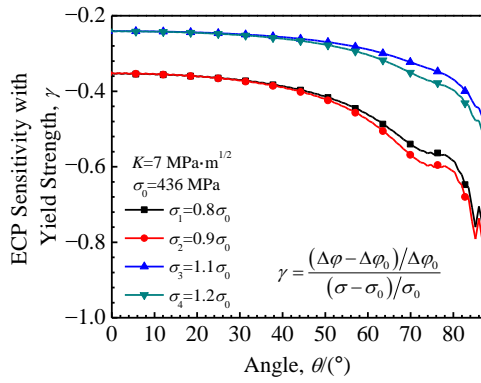


Fig.7 Sensitivity of ECP changes with yield strength

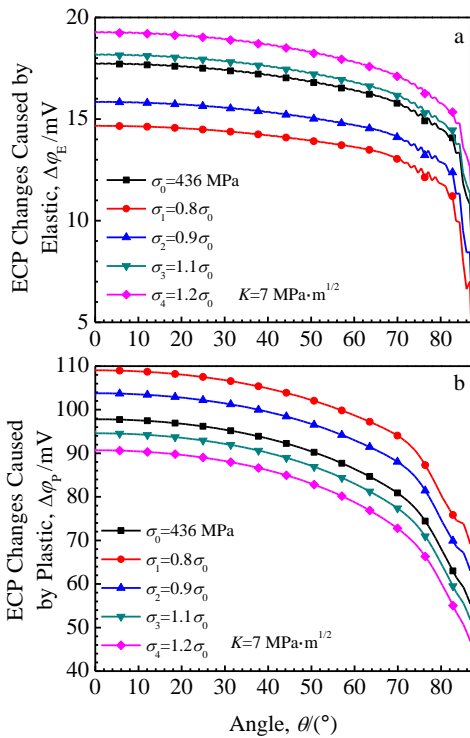


Fig.8 ECP changes on crack tip surface with different yield strength: (a) elastic part and (b) plastic part

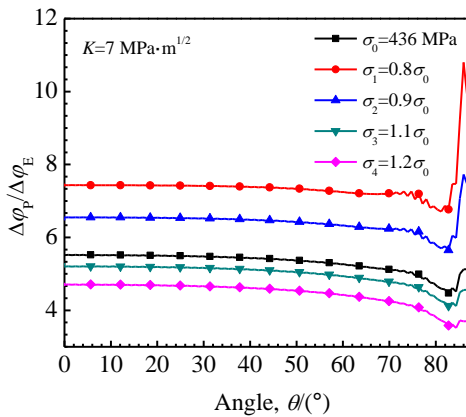


Fig.9 $\Delta\phi_P/\Delta\phi_E$ on crack tip surface under different yield strength

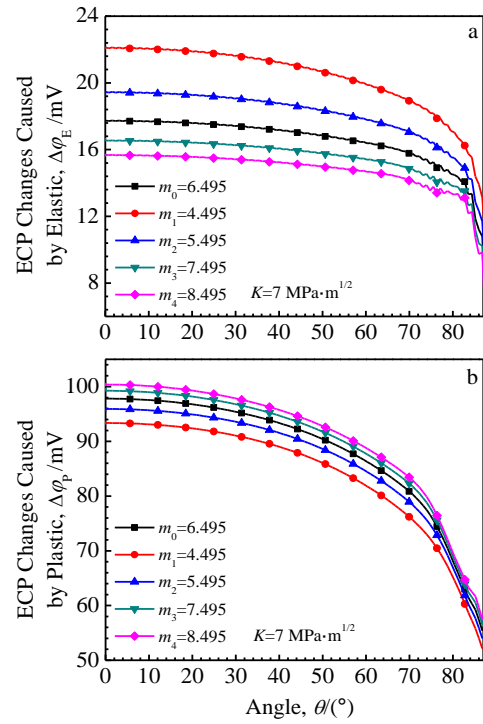


Fig.10 ECP changes on crack tip surface with different hardening exponent: (a) elastic part and (b) plastic part

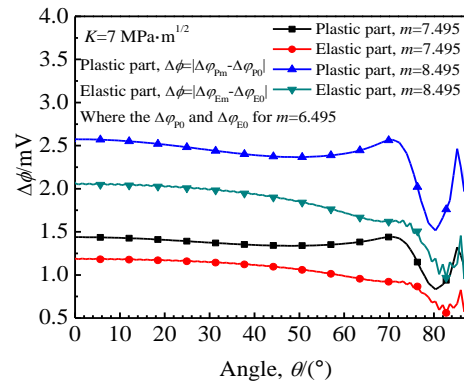


Fig.11 Comparison of ECP changes caused by elastic and plastic deformation

rapidly when θ exceeds 85° , which is mainly caused by the rapid decreasing of $\Delta\phi_E$ when $\theta > 85^\circ$. Furthermore, the value of $\Delta\phi_P/\Delta\phi_E$ decreases with increasing of yield stress.

The changes of $\Delta\phi_E$ and $\Delta\phi_P$ with different hardening exponent of alloy 600 are shown in Fig.10. The $\Delta\phi_E$ and $\Delta\phi_P$ have converse change trends when the hardening exponent of alloy 600 changes. The comparisons of $\Delta\phi_E$ and $\Delta\phi_P$ shown in Fig.11 indicate that no matter the value of hardening exponent increases from 6.495 to 7.495 or to 8.495, the differences between $\Delta\phi_E$ and $\Delta\phi_P$ are little, and this can explain that the ECP changes of crack tip surface are not obvious as shown in Fig.6b when hardening exponent changes.

4 Conclusions

1) The mechanochemical influence on crack tip surface has the maximum value at the front of the crack propagation, and decreases gradually away from the front of the crack propagation; the smallest value appears at the sides of crack tip.

2) The variation of material properties will not change the distribution trends of ECP changes on crack tip surface, but the value of ECP change decreases with increasing of yield strength of alloy 600. The influence of hardening exponent change of alloy 600 on the ECP change at crack tip surface is insignificant.

3) The sensitivity of ECP to the yield strength around crack tip surface has the lowest value at the front of crack, while the strongest sensitivity appears at the sides of crack tip. The distribution of ECP has low sensitivity with the increase or the decrease of amplitude of yield strength, but the decrease of yield strength will affect the ECP value more evidently than the increase of yield strength.

References

- 1 Hwang S S, Kim H P, Lim Y S et al. *Corrosion Science*[J], 2007, 49: 3797
- 2 Rebak R. In: Shipilov S A ed. *Environment Induced Cracking of Metal-2*[C]. Elsevier, 2008: 435
- 3 Ford F P. *International Journal of Pressure Vessels and Piping* [J], 1989, 40: 343
- 4 Hoffmeister H, Klein O. *Nuclear Engineering and Design*[J], 2011, 241: 4893
- 5 Xue H, Xue X F, Tang W et al. *Rare Metal Materials and Engineering*[J], 2011, 40(6): 1188 (in Chinese)
- 6 Yamazaki S, Lu Z P, Ito Y et al. *Corrosion Science*[J], 2008, 50: 835
- 7 Gutman E M. *Mechanochemistry of Solid Surfaces*[M]. London: Word Scientific Publishing Co Pte Ltd, 1994
- 8 Xu L Y, Cheng Y F. *Corrosion Science*[J], 2012, 59: 103
- 9 Xu L Y, Cheng Y F. *Corrosion Science*[J], 2012, 64: 145
- 10 Xue H, Shi Y W. *International Journal of Pressure Vessels and Piping*[J], 1998, 75: 575
- 11 Xue H, Ogawa K, Shoji T. *Nuclear Engineering and Design*[J], 2009, 239: 628
- 12 Zhao L Y, Xue H, Tang W et al. In: *ASME 2011 Pressure Vessels and Piping Conference Vol. 3: Design and Analysis*[C]. USA: ASME, 2011: 223
- 13 ASTM Standard E399-90. *Annual Book of ASTM Standards*[M]. USA: ASTM International, 2002
- 14 Ramberg W, Osgood W R. *Description of Stress-Strain Curves by Three Parameters, No 902*[R], USA: NACA Tech Note, 1943
- 15 Yang F Q, Xue H, Zhao L Y et al. *Rare Metal Materials and Engineering*[J], 2014, 43(3): 513
- 16 Panter J, Viguier B, Cloué J M et al. *Journal of Nuclear Materials*[J], 2006, 348(1-2): 213
- 17 Guo H X, Lu B T, Luo J L. *Electrochemistry Communications*[J], 2006, 8: 1092

高温水环境中镍基合金力学性能对裂尖力学化学效应的影响

杨富强, 薛 河, 赵凌燕, 方秀荣
(西安科技大学, 陕西 西安 710054)

摘 要: 力学与化学相互作用引起的力学化学效应会加速核电站中镍基合金的应力腐蚀开裂行为。焊接接头材料力学性能的不均匀性, 将间接影响材料的力学化学效应。采用标准紧凑拉伸试样和有限元方法, 研究得到了高温水环境中600合金屈服强度和硬化指数对裂纹尖端表面力学化学效应的影响, 分析了弹性和塑性变形对裂纹尖端力学化学效应的作用。结果表明, 600合金裂尖表面的力学化学效应受到屈服强度变化的影响, 但硬化指数对裂尖表面力学化学效应的影响不明显。

关键词: 力学化学效应; 屈服强度; 硬化指数; 裂尖; 有限元

作者简介: 杨富强, 男, 1982年生, 博士生, 西安科技大学理学院, 陕西 西安 710054, 电话: 029-83856250, E-mail: yang_afreet@163.com